

Site-Specific Patterns of Articular Cartilage Surface Damage Imply Progressive States of Degeneration during Development of Post-Traumatic Osteoarthritis in ACL-Transsected Rabbit Knees

Alborz Jelvani¹, Nasim Eshragh Nia¹, Gaya Kalyan¹, Alana T Yee¹, Aileen Liao¹, Julian J Garcia¹, Aimee R Raleigh¹, Shingo Miyazaki¹, Junichi Yamada¹, Barbara L Schumacher¹, Albert C Chen¹, Koichi Masuda¹, Robert L Sah¹

¹University of California-San Diego, La Jolla, CA, USA; ajelvani@eng.ucsd.edu

Disclosures: AJ(N), NE(N), GK(N), ATY(N), AL(N), JJG(N), ARR(N), SM(N), JY(N), BLS(N), ACC(N), KM(3B-Anges Inc; 5-Anges Inc, Kolon TGC, Inc; 6-Histogen Inc, Damatein; 8-JOR Spine, JOR, Spine J), RLS(5-Restoration Biologics; 6-JRF Ortho; 8-Cartilage, Osteoarthritis & Cartilage)

INTRODUCTION: After knee destabilizing anterior cruciate ligament (ACL) injury, joint mechanics are altered and post-traumatic osteoarthritis (PTOA) often ensues. ACL rupture leads to increased anterior translation and internal rotation of tibia, causing specific regions of femoral condyle (FCs) articular cartilage (AC) to be exposed to increased sliding (Fig 1A) and loading (Fig 1B). While traditional histopathological analysis of vertical tissue sections indicates that surface fibrillation and fissures can progress to tissue erosion,¹ how joint pathomechanics leads to localized AC damage in OA is difficult to assess in such sections. AC surfaces can be analyzed by High-Resolution Digital Imaging of India Ink Stained (HiReD-IIIS) to assess surface patterns typical of damaged human AC.² In the rabbit ACL transection (rACLT) model of PTOA, AC deterioration occurs with erosion at 6-8 weeks.³ We **hypothesized** that early AC damage exhibits site-specific patterns consistent with altered sliding and loading. The **aims** were (1) to determine if 4 week rACLT AC damage patterns are distinct at FC locations of abnormally high loading and/or sliding, and (2) to stage patterns to identify possible pathways of progressive AC damage in PTOA.

METHODS: The effect of surgery on site-specific AC surface damage patterns for (A) non-operated normal (NL), (B) non-operated contralateral (CL), and (C) ACLT knees (N=10), were determined. **Rabbit Samples.** With IACUC approval, ten adult female New Zealand White (NZW) rabbits (11-19 mo, weight = 3.8-5.2 kg) were subjected to unilateral ACLT to induce PTOA. At day 28, rabbits were sacrificed, and the right ACLT and left CL knees were harvested. Ten adult NZW hindlimbs served as NL from a separate cohort. FCs were then exposed. **Digital Imaging & Processing.** AC surfaces were aligned, dabbed with a 1:5 dilution of India Ink in phosphate buffered saline + proteinase inhibitors, and digitally imaged at (4 µm)²/pixel. Gray-scale images were normalized to 0 (darkest) and 1 (brightest) using standards. For site-specific analysis (Fig 1C), images of lateral and medial FC (LFC, MFC) were divided into NWB and WB loading regions, and **OUT**er, **CENT**ral, and **INN**er subsites, based on FC anatomical landmarks. **Grading.** A standardized, sensitive, and reliable grading guide, supplemented with an image atlas, was developed for AC surface damage patterns identification (Fig 2 Table). Damage patterns, including **HAze** (HAZ), **Dash** (DAS), **Transverse** (TRA) Line, **Longitudinal** (LONG) Line, **Reticular Sawtooth** (RST), and **Broad Streak** (BSK), were graded within 12 FC subsites (Fig 1C) of ~4×1.5 mm². Scores for each pattern were determined. Site-specific progression pathways were deduced from decreasing incidence of pattern score. **Statistics.** Intra- and inter-observer reliability of the grading guide were determined for each pattern by three independent observers using Cohen's and Fleiss' κ, respectively. Score data are shown as mean±SE. At each FC subsite, scores of each pattern were compared (ACLT vs controls) by non-parametric Kruskal-Wallis test and Dunn's *post hoc* test. Significance was taken as p<0.05.

RESULTS: Reliability. The intra- and inter-observer agreements were high (p<0.001). Cohen's κ (intra-observer) was 0.92±0.05 (range 0.83-1.00) overall. Fleiss' κ (inter-observer, range 0.84-0.96 for all patterns) was 0.88±0.04 for original and 0.90±0.02 for repeat scores. **Damage Patterns.** Subsite LFC NWB OUT had higher scores (more damage) for all six patterns in ACLT FC (Δ=0.7±0.2) compared to NL (Fig 3), with similar trends at LFC WB OUT, except BSK were higher in ACLT FC (Δ=0.6±0.2). Subsite LFC WB INN had higher scores for all patterns except HAZ in ACLT FC (Δ=0.7±0.2) compared to NL. At MFC WB OUT, ACLT FC had higher scores for all patterns except TRA compared to NL (Δ=0.5±0.1). **Pattern Stage.** At LFC OUT, all six patterns were co-localized with grade 1 RST. At WB INN LFC and OUT MFC, HAZ, DAS, RST (grade 2), and BSK were co-localized.

DISCUSSION: Presence of different combinations of DAS, TRA, LONG, RST, and BSK at OUT and INN subsites imply possible degeneration progression pathways and damage mechanisms (Figs. 1,2G). Consistent with knee translational and rotational instability after ACLT, prevalence of patterns at peripheral NWB and WB regions of LFC (Fig. 2G [S1-4]) suggests potential stress concentration sites due to excessive sliding between FC AC-menisiscus in OUT subsites (Fig. 1A). Abnormally high compressive loading between FC AC-tibial AC and -tibial spine in INN subsite of WB LFC, and between FC AC-menisiscus in OUT subsite of WB MFC (Fig. 1B), may derive a distinct AC damage progression pathway (Fig. 2G [L1-4]).

SIGNIFICANCE: The identification of *en face* AC damage patterns may provide opportunities for more targeted early treatments. The recognition of patterns of AC damage at sites subjected to more sliding or more loading indicates distinct biomechanical mechanisms by which instability contributes to PTOA.

REFERENCES: [1]Pritzker K+, *Osteoarthritis Cartilage*, 2006.[2]Jelvani A+, *Trans Orthop Res Soc*, 2020. [3]Yoshioka M+, *Osteoarthritis Cartilage*, 1996.

FIGURES AND TABLES:

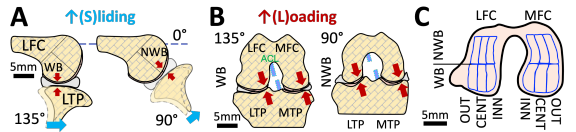


Fig 1. Hypotheses. (A) Sliding. (B) Loading. (C) Areas analyzed.

#	PATTERN	GRADE	EXTENT	DEFINITION	A	B	C	D	E	F
1	HAze	0,1	<20%, ≥20%	Patches of gray	1	0	1	1	1	1
2	DASH	0,1	<5 / area, ≥5 / area	Lines, length ≥100 µm	1	0	1	1	1	1
3	TRANSverse	0,1	<1 / area, ≥1 / area	Lines, length ≥250 µm, 0-45° to horizontal	0	1	1	1	1	1
4	LONGitudinal	0,1	<1 / area, ≥1 / area	Lines, length ≥250 µm, 45-90° to horizontal	0	0	1	1	1	0
5	Reticular Sawtooth	0,1,2	<20%, ≥20%	Lines, length ≥100 µm, interconnected	0	0	0	1	2	0
6	Broad Streak	0,1	<1 / area, ≥1 / area	Patches of black, width ≥150 µm	0	0	0	0	1	1

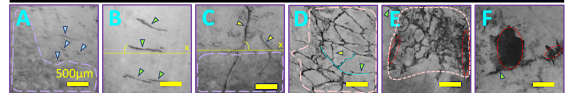


Fig 2. *En face* damage pattern grades and (A-F) examples. (G) Pathways of progressive surface damage.

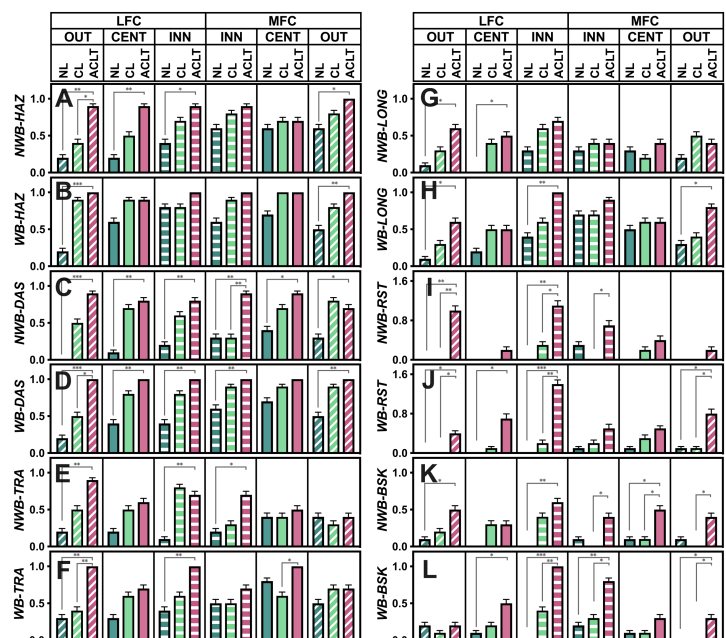


Fig 3. Site-specific damage patterns scores. *p<0.05, **p<0.01, *** p<0.001.